PROBLEMY KOLEJNICTWA
RAILWAY REPORTS Issue 183 (June 2019) ISSN 0552-2145 (print) ISSN 2544-9451 (on-line)

Droppers' Stiffness Influence on Dynamic Interaction Between the Pantograph and Railway Catenary

Danuta BRYJA[1], Adam HYLIŃSKI (POPIOŁEK)[2]

Summary
Droppers connecting the contact wire and messenger wire of the railway catenary are characterized by zero or negligible compressive stiffness, hence they become slack under compression that is similar to bars' buckling. The paper presents a numerical analysis of the influence of droppers slackening phenomenon on the dynamic interaction between the pantograph and catenary. The analysis is based on a simulation method presented by the authors in previous papers, in which the catenary is modelled as a complex cable system. In this paper, the simulation method is modified by introducing the residual compressive stiffness of droppers that is assumed as a given percent of tensile stiffness. Modification leads to geometrically non-linear equations of motion of the pantograph-catenary system. Two different algorithms for solving the problem of non-linearity are proposed, in both of them the Newmark numerical integration method is applied. Results of dynamic response simulations performed for different values of residual compressive stiffness of droppers are presented and compared. It is shown that the contact wire does not cooperate with the messenger wire in a large area around the pantograph when the compressive stiffness of droppers is assumed zero. As a result, the pantograph moving at high speed induces severe vibrations of the catenary. It is also shown that droppers should be designed to have the residual compressive stiffness equal to at least one percent of their tensile stiffness. This is sufficient to ensure an appropriate cooperation between messenger wire and contact wire, which is demonstrated by simulation results fulfilling requirements given in the standard PN-EN 50318: 2002.

Keywords: railway catenary, pantographs, droppers' slackening, geometrical non-linearity, vibration simulation, validation of simulation method

1. Introduction

In recent years, a growing interest in numerical methods for simulation of dynamic interaction between railway catenary and moving pantographs can be observed in global [6, 11, 13] and Polish literature [9, 14]. More and more advanced simulation methods are being proposed, which increasingly well reflect real catenary operational conditions. However, in most cases authors apply a similar approach assuming the FEM modelling of all catenary structural elements (messenger wire, contact wire, droppers, steady arms, support structures), with the use of Euler's beam elements [13]. Such an approach takes into account the flexural stiffness of messenger wire and this of contact wire, which are negligible while considering the fact that the length of the multi-span catenary is many times bigger than characteristic cross-sections of both wires. At the same time, such an approach ignores a specific nature of vibrations of the catenary which constitutes a complex cable system. That will be shown below in the numerical part of this paper.

A counterfactual catenary modelling method based on the vibration theory of flexible cables and the Lagrange – Ritz method has been proposed by the authors of this paper. The first version of the method was published in [5] where a detailed description of the computational model for the pantograph-catenary system is presented including a step-by-step derivation of equations of motion. The proposed model assumes that droppers connecting the multi-span messenger wire and the contact wire are zero-mass elastic elements which transfer tensile forces but do not transfer a compression. They behave therefore as non-linear

[1] Prof. Ph.D. Eng.; Wroclaw University of Science and Technology, Faculty of Civil Engineering, Department of Bridges and Railways; e-mail: danuta.bryja@pwr.edu.pl.
[2] M.Sc. Eng.: Wroclaw University of Science and Technology, Faculty of Civil Engineering, Department of Bridges and Railways; e-mail: adam.hylinski@pwr.edu.pl.

springs of the "stop" type [7], which have different stiffness (non-zero and zero, respectively) depending on the relative displacement of both spring ends.

The phenomenon of non-transferring the compressive forces by droppers arises from their design. They are usually flexible cords made of individual copper wires – for example, the catenary utilised by PKP uses droppers of the L10 type with a cross-section of 10 mm^2, with double strand 7×7 wires having a nominal diameter of 0.51 mm. Under compressive forces, such cords lose their shape – they become slack which is similar to bar buckling. During the pantograph passage, the contact wire moves up at a contact cross-section and a certain distance away from it, which is due to the contact force exerted by the pantograph head. Simultaneously, lower ends of droppers move up causing droppers' slackening, that results in a temporary disconnection of the messenger wire and the contact wire, near the contact cross-section. Then, after the pantograph passage, the contact wire moves alternately down and up experiencing free vibrations. Each down movement tenses droppers and causes a return to the state in which the contact and messenger wires are connected.

Taking the described phenomena into account in the catenary computational model leads to a geometrically non-linear problem, consequently, the numerical integration scheme of the equations of motion becomes more complicated. The authors have proposed in [2] a method for solving non-linear equations of motion, which is based on an iterative determination of the non-linear forces compensating the influence of droppers up to zero, for the droppers which are identified as subjected to compression in a given calculation step. Identification of such droppers is performed on the basis of an observation of the relative displacement of both ends of each dropper. The compressive stiffness of slackening droppers equals zero if the compensating forces are determined with an appropriate accuracy. A similar approach was used by Pombo in [1, 13] where it is suggested, without precise analysis, that the compensating forces should be calculated in such a way to leave the residual compressive stiffness of droppers.

Regarding the above, the main aim of this paper was defined as an analysis of the influence of the droppers residual compressive stiffness on the dynamic interaction between the pantograph and railway catenary. The analysis is based on a previously elaborated simulation method, modified to consider the residual compressive stiffness of droppers which become slack. This residual stiffness is defined as an appropriate percent of dropper tensile stiffness, which will be achieved by step-by-step reduction of the initial value equal to tensile stiffness. Within the first step of the analysis, dynamic responses of the pantograph-catenary system are determined for different values of the dropper compressive stiffness: from initial value characteristic for the tensile mode (zero stiffness reduction for compression, all droppers are linearly elastic regardless of their relative displacements) to zero (complete stiffness reduction). The second step of the analysis takes into account cases when the dropper compressive stiffness is equal to a low percentage of initial (tensile) value. Such highly reduced stiffness reflects the residual compressive stiffness which can be applicable for droppers subjected to slackening [1]. For the purpose of verification of the obtained results, an alternative procedure for solving the non-linear equations of motion is elaborated and the results obtained by both algorithms of the simulation method are compared.

The obtained results show that assuming droppers' compressive stiffness equal to zero, in the case when the catenary model is based on a flexible cable theory, significantly influences dynamic responses of the pantograph-catenary system. For high pantograph speeds, the contact wire practically does not cooperate with the messenger wire and experiences significant vibrations. It is shown that assuming the residual compressive stiffness equal to one percent of tensile stiffness is adequate for ensuring an appropriate cooperation between the both wires of catenary, which is demonstrated by simulation results fulfilling standard requirements [12].

2. Simulation method

The computational model of pantograph-catenary system, as well as the method for simulating the dynamic interaction between the overhead contact line and moving pantographs, which are utilised in numerical analysis presented in this paper, have been precisely described and tested by the authors in [2–5]. All numerical tests presented in those papers were conducted with a simplified versions of the simulation method. In [2], which was dedicated to the influence of damping on the dynamic system response, simplification was based on the assumption that droppers are linearly elastic springs – i.e. they transfer both compressive and tensile forces. Two works [3, 4], take the non-linear behaviour of droppers into account but only one iterative step is used in the procedure applied for calculating a vector of non-linear forces compensating the influence of droppers subjected to compression. This simplified variant was used in [12] to conduct an initial validation of the simulation method, in accordance with standard requirements [4]. Such validation is necessary in order to accept use of the elaborated method in engineering practice. In turn, the paper [3] presents an example of pantograph-catenary system vibration analysis in the case of two moving pantographs.

This work utilises the full version of the simulation method described in [2], which is based on the computational model presented in [5]. The mathematical description of the method is slightly modified in order to enable the goal of the research to be achieved. General catenary model assumptions are the same as in [5], i.e.: (*i*) the catenary consists of one contact wire and one messenger wire (see Fig. 1), (*ii*) the catenary section being analysed is composed of a given number of spans, (*iii*) the multi-span messenger wire is represented by a flexible cable with a parabolic route within each individual span (in an unloaded state), and is slidingly supported on rigid supports, (*iv*) the contact wire is treated as a straight cable (i.e. string). Both the messenger and contact wire are tensed, which is provided by special devices dedicated for catenary tensioning.

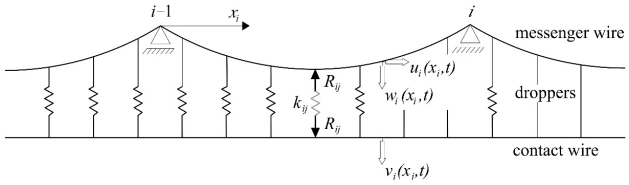

Fig. 1. Railway catenary scheme [own study]

The contact wire is suspended to messenger wire by flexible droppers which are modelled by non-linear springs of the stiffness k_{ij}. The subscript *i* refers to the span number, while *j* denotes the dropper number in the i^{th} span. The tensile stiffness k_t of all droppers is identical, constant and equal to *k*. Compressive stiffness k_c is also identical for all droppers, constant and equal to κk, where κ is a coefficient which determines the part of stiffness *k* remaining after the assumed droppers stiffness reduction applicable for the droppers being compressed. Assuming $\kappa = 0$ means full reducing stiffness to zero (droppers have zero compressive stiffness), $\kappa = 1$ means a lack of reduction (compressive stiffness is the same as tensile stiffness). In the following part of this paper, the κ coefficient is given in percentage and named shortly the compressive stiffness, and its small values are named the residual compressive stiffness.

The rule adopted for determining the dropper stiffness can be written by the following conditional definition

$$k_{ij} = \begin{cases} k_t = k \quad \text{gdy} \quad R_{ij}(t) - R_{ij}^0 \le 0 & \text{(dropper under tension)} \\ kc = \kappa k \quad \text{gdy} \quad R_{ij}(t) - R_{ij}^0 > 0 & \text{(dropper under compression)} \end{cases} \tag{1}$$

which means that, in this paper, the droppers are modelled by bilinear springs [7]. While using equation (1), it is important to remember that the force $R_{ij}(t)$ denotes the dynamic reaction of the spring – positive when directed as it is shown in Fig. 1. At the same time, the spring is loaded by inversely directed forces, that is – compressive forces. Therefore, the dropper is compressed when $R_{ij} - R_{ij}^0 > 0$. The force $R_{ij}^0 = m_p g d_{ij}$ represents the spring reaction caused by the dead weight of the contact wire, where m_p is the mass per unit length of the wire, *g* gravitational acceleration, and d_{ij} distance between droppers. The time-dependent spring reaction is given by

$$R_{ij}(t) = k_{ij}[w_i(x_{ij},t) - v_i(x_{ij},t)] \tag{2}$$

in which $w_i(x_{ij},t)$ and $v_i(x_{ij},t)$ mean vertical displacements of the messenger wire and the contact wire, respectively, in the place of dropper clamping x_{ij} (see Fig. 1). Definitions (1) and (2) show that the stiffness of each dropper depends on the current state of motion of the messenger wire and of the contact wire, causing the geometrical non-linearity of equations of motion of the catenary.

The contact wire is loaded by one or two pantographs moving with a constant speed at a fixed distance between each other. Pantographs are modelled as two-degrees-of-freedom systems, in which mass elements represent the collector head and articulated frame (see Fig. 2). These elements are linked by linear springs and viscous dampers. In static conditions, the pantograph acts on the catenary with the constant uplift force $F = F_1 + F_2$, which is, in dynamic conditions, complemented by the dynamic increment $P_J(t)$, giving the cumulative contact force $R_J(t)$, where *J* is a pantograph number. A contact elastic connection (spring) is used between the pantograph and contact wire. Such an element does not exist physically within the pantograph-catenary system, but using it simplifies determination of the current contact force and is permitted by standard [12].

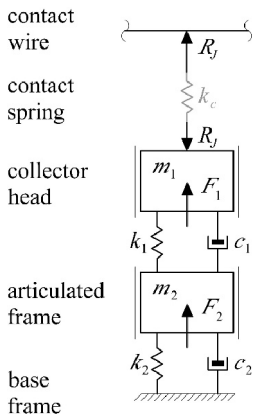

Fig. 2. Pantograph dynamic model [own study]

The equations of motion of the pantograph-catenary system, derived in [5] and written in the matrix notation, have the following general form:

$$\mathbf{B}\ddot{\mathbf{q}}(t)+\mathbf{C}\dot{\mathbf{q}}(t)+\mathbf{K}(t)\mathbf{q}(t)=\mathbf{f}(t) \tag{3}$$

Among the characteristic matrices of the equation (3), the stiffness matrix $\mathbf{K}(t)$ is the most important from the non-linear dropper behaviour viewpoint. Similarly to that in [9], it is subdivided into four components as follows

$$\mathbf{K}(t)=\mathbf{K}_{\text{const}}+\hat{\mathbf{K}}_{\text{const}}-(1-\kappa)\hat{\mathbf{K}}_{\text{ws}}(q)+\tilde{\mathbf{K}}(t) \tag{4}$$

where the components $\mathbf{K}_{\text{const}}$ i $\hat{\mathbf{K}}_{\text{const}}$ are constant matrix, and component $\tilde{\mathbf{K}}(t)$ varies in time because depends on dynamic interaction between the catenary and pantographs. The matrix $\mathbf{K}_{\text{const}}$ depends only on the elastic characteristics of the multi-span messenger wire and contact wire, while the separated component $\hat{\mathbf{K}}_{\text{const}}$ contains all these elements of the general stiffness matrix which depend on the dropper stiffness. The matrix $\hat{\mathbf{K}}_{\text{const}}$ is calculated with an assumption that all droppers have non-zero initial stiffness k, both for tension as well as for compression. The component $\hat{\mathbf{K}}_{\text{ws}}(\mathbf{q})$ has the same structure as $\hat{\mathbf{K}}_{\text{const}}$, but is dedicated only to droppers which are identified as being compressed at the t moment. It is therefore dependent on the general coordinates $\mathbf{q}(t)$ describing the motion of the catenary-pantographs system. It is easy to notice that the result of subtraction operation: $\hat{\mathbf{K}}_{\text{const}}-(1-\kappa)\hat{\mathbf{K}}_{\text{ws}}(\mathbf{q})$, occurring in relation (4), reduces the compressive stiffness of droppers to the value $k_c = \kappa k$. Identification of the droppers being compressed is performed in each time step h of the numerical integration of equations of motion. For numerical integration of equation system (3), the unconditionally stable variant of the Newmark method is applied.

Taking into account the internal structure of the stiffness matrix (4) makes possible to rewrite the equation system (3) in two alternative forms

$$\begin{aligned}&\mathbf{B}\ddot{\mathbf{q}}(t)+\mathbf{C}\dot{\mathbf{q}}(t)+[\mathbf{K}_{\text{const}}+\hat{\mathbf{K}}_{\text{const}}+\tilde{\mathbf{K}}(t)]\mathbf{q}(t)=\\&=\mathbf{f}(t)+(1-\kappa)\hat{\mathbf{K}}_{\text{ws}}(\mathbf{q})\mathbf{q}(t)=\mathbf{f}(t)+\mathbf{f}_{\text{nl}}(\mathbf{q})\end{aligned} \tag{5}$$

$$\begin{aligned}&\mathbf{B}\ddot{\mathbf{q}}(t)+\mathbf{C}\dot{\mathbf{q}}(t)+\\&+[\mathbf{K}_{\text{const}}+\hat{\mathbf{K}}_{\text{const}}-(1-\kappa)\hat{\mathbf{K}}_{\text{ws}}(\mathbf{q})+\tilde{\mathbf{K}}(t)]\mathbf{q}(t)=\mathbf{f}(t)\end{aligned} \tag{6}$$

which constitute a basis of two alternative algorithms of the simulation method.

The first algorithm, based on equation (5), is similar to one described in [9]. Taking into account the relation (4), it is easy to distinguish from the equation (3) the non-linear component $\mathbf{f}_{\text{nl}}(\mathbf{q})=(1-\kappa)\hat{\mathbf{K}}_{ws}(\mathbf{q})\mathbf{q}(t)$ and move it to the right side, pairing it with the vector $\mathbf{f}(t)$ representing excitation forces. The component $\mathbf{f}_{\text{nl}}(\mathbf{q})$ is a vector gathering unknown non-linear forces which reduce the compressive stiffness of droppers to the value $k_c = \kappa k$. It is estimated in the iterative loop in each step of the numerical integration, up to the required accuracy. In the first iterative step, the vector $\mathbf{f}_{\text{nl}}(\mathbf{q})$ is determined on the basis of solution of the linearized collocation condition of the Newmark method [10] which is achieved simply by removing the non-linear vector $\mathbf{f}_{\text{nl}}(\mathbf{q})$.

In the second algorithm, based on equation (6), the direct correction of the stiffness matrix takes place in each calculation step of the numerical integration. This correction is performed by subtracting the component $\hat{\mathbf{K}}_{\text{ws}}(\mathbf{q})$ calculated in a current state, that is, taking into account only these droppers which are subjected to compression in a t moment. Such correction is repeated several times in a given time step, up to the required accuracy of the solution vector $\mathbf{q}(t)$. As in the first algorithm, the linearized collocation condition is used in the first iterative step.

Numerical analysis described below in this paper has been conducted utilising the both versions of simulation method, which differ in the algorithm used to obtain the non-linear solution of the system of equations of motion (3). The method based on the iterative-recurrent solution of the equation (5) is marked below by the MI symbol, while the method based on correction of the stiffness matrix in accordance with equation (6) is marked by the MK symbol.

3. Initial data and results of the numerical analysis

The physical parameters of the pantograph – catenary system, which were taken for calculations, are shown in Table 1. They were adopted mainly on the basis of the data representing the reference model described in standard [12], which is dedicated to validation of simulation methods. Other catenary characteristics result from the tests conducted in earlier stages of authors' research, described in [2].

All simulations have been conducted assuming a catenary load by a passage of one pantograph at the speed of 300 km/h. The total length of the tested catenary section, composed of five identical spans, was 300 m. On the basis of authors experience, such a section length is sufficient to examine a quality of simulation results and for an initial quantity analysis. A thorough quantity analysis would require to adopt a longer catenary section, composed of minimum of ten spans [12].

Table 1

Geometrical and materials characteristics of the catenary structural elements and parameters of the pantograph

Catenary system		Pantograph	
Messenger wire specific mass [kg/m]	1.07	Speed of the pantograph [km/h]	300
Messenger wire tension [kN]	16	Mass of the pantograph head [kg]	7.2
Messenger wire axial stiffness [MN]	12	Mass of the pantograph frame [kg]	15.0
Contact wire specific mass [kg/m]	1.35	Pantograph static force [N]	120
Contact wire tension [kN]	20	Stiffness of the upper spring of the pantograph [N/m]	4 200
Dropper tensile stiffness [kN/m]	100	Stiffness of the lower spring of the pantograph [N/m]	50
Span length [m]	60	Parameter of the upper damper of the pantograph [Ns/m]	10
Number of spans	5	Parameter of the lower damper of the pantograph [Ns/m]	90
Number of droppers within span	9	Stiffness of the contact spring [kN/m]	50
Material damping coefficient of the messenger wire [%]	0.5	–	

Numerical analysis has been divided into two parts. In the first part, tests were conducted by the use of the first simulation method (MI), namely with an iteration of the non-linear forces compensating an influence of the droppers being compressed, assuming the time step length for numerical integration: $h = 0.001$ s. The aim of those tests was to analyse the influence of the compressive stiffness of droppers on the system dynamic response. In the second part, the results obtained by both methods were compared (MI and MK), assuming the integration step $h = 0.001$ s and $h = 0.0001$ s. Among others, that enabled a more effective method to be indicated.

Figure 3 shows the simulation results obtained for six different values of the compressive stiffness of droppers: from $k_c = 100\%k$ ($\kappa = 100\%$, no reduction, dropper compressive stiffness equals tensile stiffness) to $k_c = 10\%k$ ($\kappa = 10\%$, reduction to 10%). In Fig. 3a, time histories of the contact wire vibrations at the right steady arm of the middle catenary span are shown. The observation time starts from the pantograph entry, and covers a whole passage over the tested catenary section, together with free vibrations which occur after the pantograph leaves the section. Time histories of the pantograph head vibrations and dynamic changes in the contact force, during the pantograph passage over two middle catenary spans (third and fourth), are presented in Figure 3b and Figure 3c, respectively. The horizontal axis has been scaled to match the distance between the vertical lines of the chart grid with a time interval which corresponds to the pantograph passage over a single span. Negative values of the contact wire displacement or pantograph head displacement mean an uplift.

Comparison of the presented time histories shows that changes in the droppers compressive stiffness, in the examined range, have a negligible influence on the contact wire uplift at the steady arm. A slightly bigger influence is observed in the case of pantograph head vibrations – an increase in the uplift of pantograph head together with a decrease in the compressive stiffness of droppers is a general tendency. Changes are not large (do not exceed 10% of the maximum values), but they significantly influence the contact force. In this case, the differences in time histories are significant.

It follows from Figure 3b that a lack of reduction in the compressive stiffness of droppers ($k_c = 100\%$) results in large peaks of the contact force oscillations. Even peaks with negative values are observed, that has to be interpreted as a loss of contact between the pantograph head contact strip and contact wire, which results not only in unacceptable breaks in power supply but also in arcing leading to damages on the contact surfaces. Reduction in the droppers compressive stiffness positively influences the contact force, however, a significant mitigation of the oscillation amplitudes occurs for the lowest stiffness only ($k_c = 100\%$).

In order to establish how the system reacts when the compressive stiffness is even lower, the second stage of an analysis was conducted. A higher reduction in the dropper compressive stiffness was examined, namely the reduction to the values: $k_c = 1\%, 0.1\%, 0\%$, wherein the values of the order of 1% and 0.1% describe the residual compressive stiffness of droppers. Simulations of dynamic responses of the system, executed in the above cases, have been compared with the solutions obtained for the previous range of droppers compressive stiffness. Selected results are shown in Figure 4.

The residual stiffness of the order of 1% gives the results which do not differ significantly from the ones obtained for the stiffness of 10%. In contrast, the residual stiffness value of 0.1% leads to a significant, nearly double increase in the maximum uplift of the contact wire (see Fig. 4a), while the contact force os-

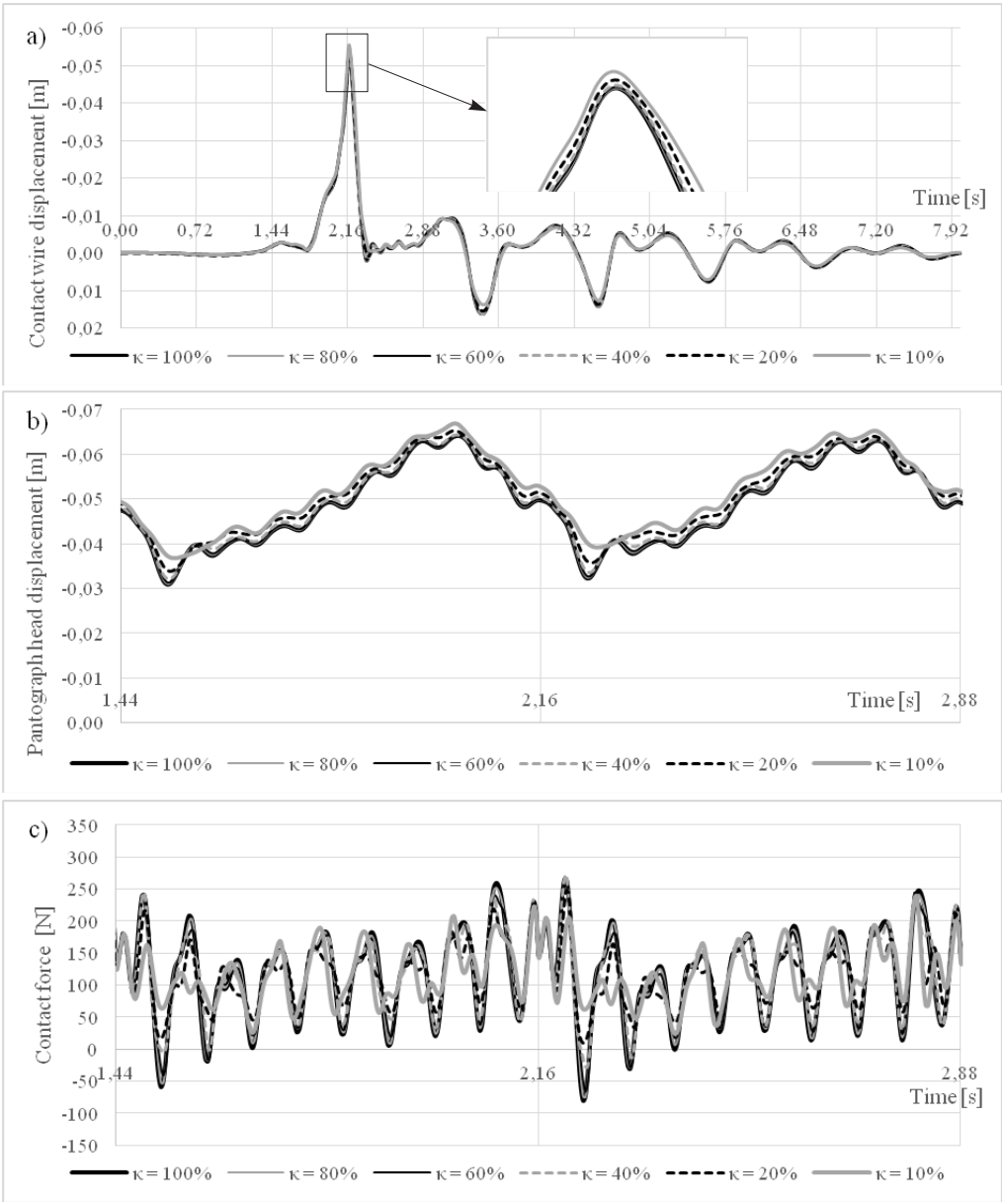

Fig. 3. Time histories: a) contact wire uplift at the right steady arm of the middle catenary span, b) displacement of the pantograph head, c) contact force, depending on the compressive stiffness of droppers [own study]

cillations do not decrease in a substantial way (see Fig. 4b). Reducing stiffness to zero, which is suggested by the standard [12] for the reference model, on one hand, gives generally lower oscillations of the contact force, but, on the other hand, results in very large maximum uplift of the contact wire. We can observe more than five times exceeding the permissible uplift range (55 to 65 mm), which is given for the reference model in the standard [12] where the results have been validated by measurements performed for typical railway catenaries. This will be explained below in the last paragraph of this chapter.

In order to check the accuracy of the calculations and verify the obtained results, analogical vibration simulations were performed for the same section of the tested catenary. However, this time the second version of the simulation method was applied (MK), consisting in corrections of the stiffness matrix in each calculation step. Time histories of the contact wire dynamic displacement at the right steady arm of the middle span, generated by both methods: MI and MK, are compared in Figure 5. The presented results were obtained with the use of the time step $h = 0.001$ s. The comparison shows that, together with lowering of

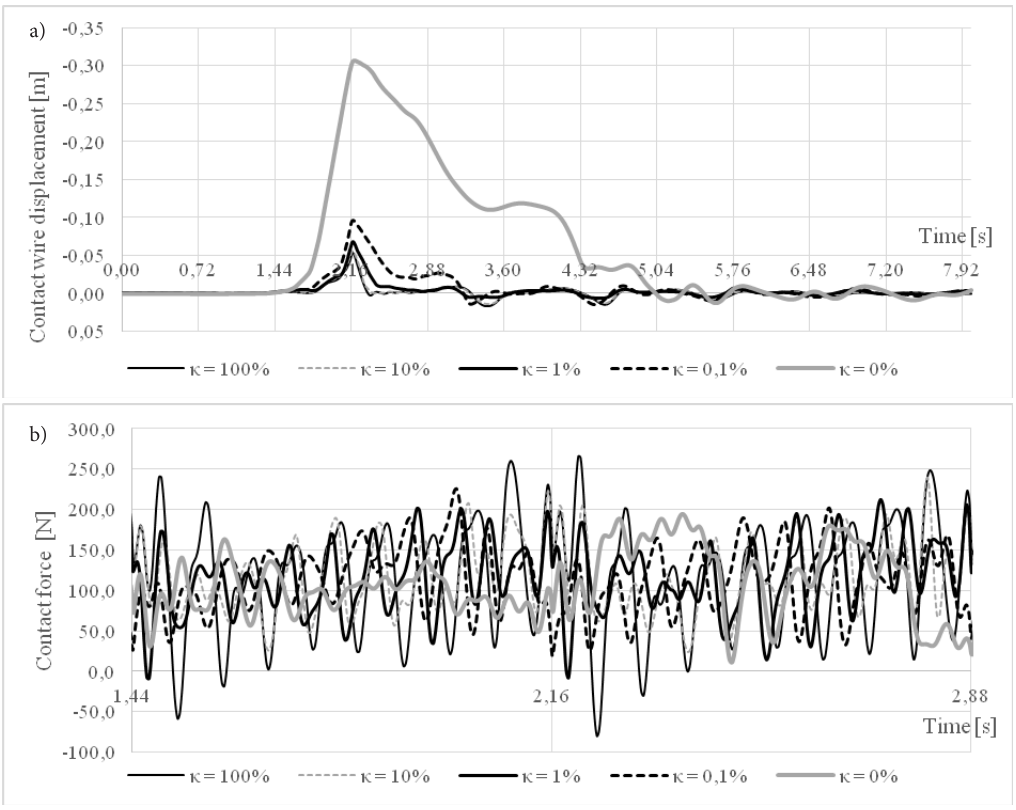

Fig. 4. Time histories: a) contact wire uplift at the right steady arm of the middle catenary span, b) contact force, depending on the compressive stiffness of droppers [own study]

the compressive stiffness of droppers, discrepancies between the results obtained by the two methods used for calculations grow. In the case of zero compressive stiffness, the MK method gives a bigger maximum uplift of the contact wire than the MI method. Moreover, the use of two methods result in a different shape of the response decaying.

Applying a smaller time step of numerical integration in the MI method: $h = 0.0001$ s leads to a high conformance of time histories obtained by both methods. This is shown in Figure 6. In the case of contact wire uplift, conformance is nearly total (see Fig. 6a). In the case of contact force, minor discrepancies can be seen in time histories corresponding to the value $\kappa = 1\%$ (see Fig. 6b).

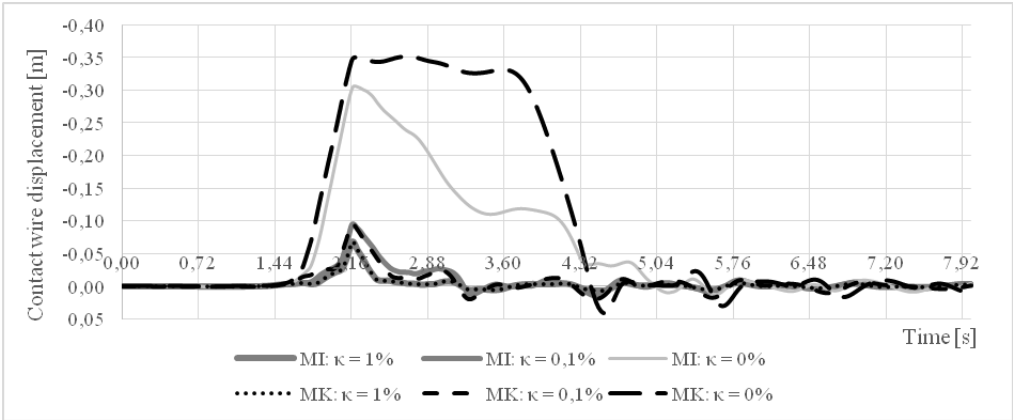

Fig. 5. Time histories of contact wire uplift at the right steady arm of the middle catenary span, generated by numerical integration with the step $h = 0.001$ s [own study]

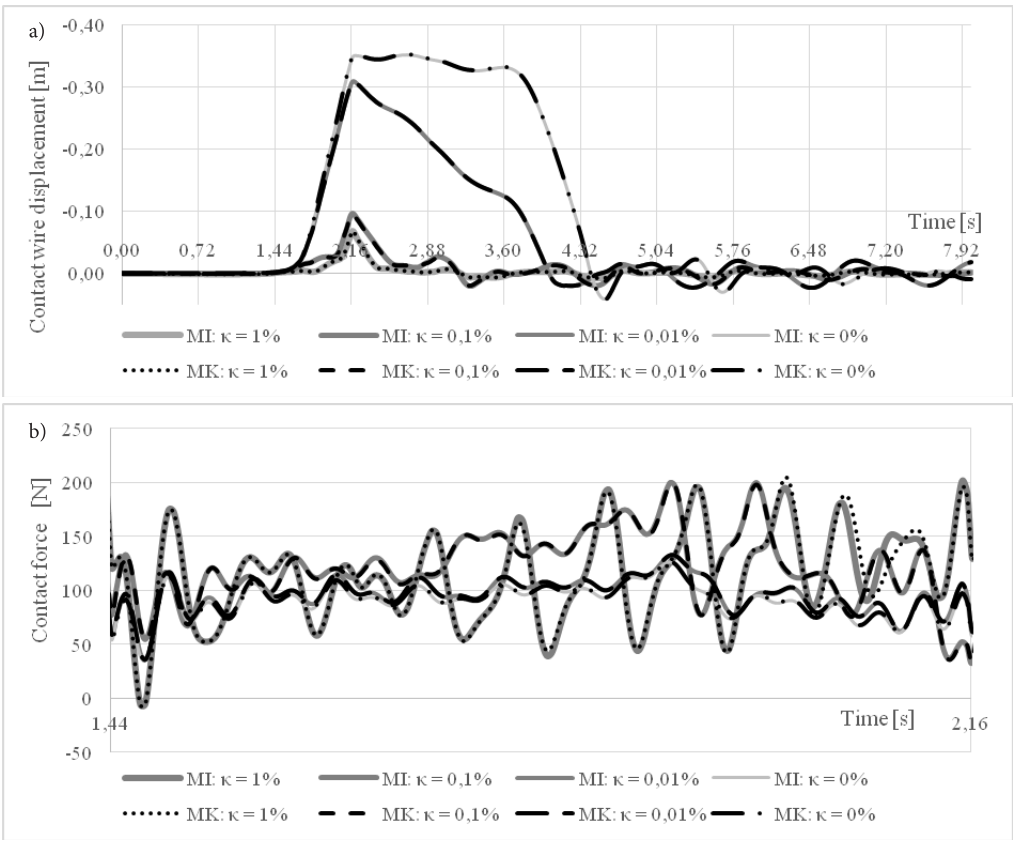

Fig. 6. Time histories: a) contact wire uplift at the right steady arm of the middle catenary span, b) contact force, generated by numerical integration with the step h = 0.001 s in the MK method and with the step h = 0.0001 s in the MI method [own study]

It is worthy to note that the computational time necessary for simulations by using the MK method is many times shorter than for the MI method, while maintaining the same accuracy. This results from the ten times lower number of time steps and from a significantly lower number of iterative steps necessary to achieve non-linear solution in each calculation step. The MK method requires 1 to 2 iterative steps while the MI method requires 5 to 8 steps. Therefore, considering the computational effort needed to obtain precise results of simulations, the MK method with the time step h = 0.001 s should be recommended for further calculations.

Within the set of simulations shown in Figure 6, there are additional time histories corresponding to the residual stiffness k_c = 0.01%k. Taking those additional simulations into account in analysis demonstrates that, together with lowering of the residual compressive stiffness of droppers, solutions approach the limit case κ = 0 in which compressive stiffness equals zero. This proves the correctness of the computational algorithm. On the other hand, this shows how the pantograph-catenary system would behave if all the droppers being under compression suddenly lost their residual stiffness up to zero.

Figure 6a shows that, in the case of zero or negligible compressive stiffness of droppers, the high uplift of the contact wire is observed when the catenary is modelled consistently as a complex cable system. It can be explained by the fact that, in the considered case, a set of droppers near the contact cross-section does not operate, and in consequence, cooperation between the messenger wire and contact wire in such an area is broken. The contact wire starts to vibrate nearly as an independent (not-suspended) string loaded by a passage of the pantograph, as shown in Figure 7. During the vibration process, the contact wire moves down after its uplift, which causes a tension of slackening droppers and a restoration of the cooperation with the messenger wire. As a result, further free vibrations occur with small amplitudes around the static equilibrium state.

4. Conclusions

Interesting conclusions arise from the numerical tests presented above. First of all, adopting a catenary model based on flexible cables theory shows that, for high operational speeds of trains, temporary large oscillations of the contact wire may occur, if droppers

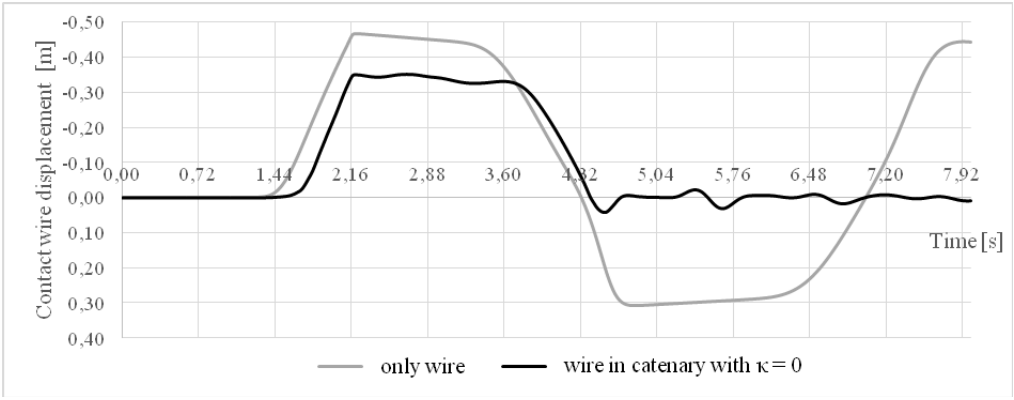

Fig. 7. Time histories of the contact wire uplift, obtained for a not-suspended wire ("only wire") and for a wire suspended to messenger wire by droppers with zero compressive stiffness ("wire in catenary with $\kappa = 0$") [own study]

compressive stiffness equals zero and droppers are initially tensed only by a self-weight of the contact wire, see equation (1). Such oscillations were observed in the past in high-speed lines, e.g. in relatively weakly tensed LN1 catenary utilised on Southeast TGV railway line [2]. They were practically eliminated, mainly by increasing the tensions of the messenger wire and contact wire in constructions built later (e.g. in LN6 catenary: to 20 kN and 26 kN, respectively). It could be supposed that an increase in the catenary tension introduces a certain initial tension of droppers, which results in their minor compressive stiffness. The presented research shows that it is sufficient to ensure a residual compressive stiffness of the order of 1% of tensile stiffness, in order to keep catenary oscillations within permitted limits.

Moreover, the presented research has shown that taking a residual compressive stiffness of droppers into account in the computational model enables simulation results to be obtained comparable with the results given in the standard [12] for the reference model. Regarding the above, a validation of the elaborated simulation method has been conducted, in accordance with the first validation step of the standard [12] but assuming one per-cent residual compressive stiffness of droppers. Calculations have been performed by the MK method with the numerical integration step 0.001 s, for the data gathered in Table 1 – with such a difference that the catenary section is composed of 10 spans, as it is required by the standard. Summary of simulation results shown in Table 2 reveals high conformance with the limits defined in the standard. Most of the parameters constituting so-called catenary dynamic characteristics are within the limits given in the standard [12]. Some, which are outside the limits, exceed them insignificantly. This

Table 2

Comparison between simulation results and limits defined in the standard

Parameter	Simulation results	Standard limits	
		min	max
Mean value of contact force F_m [N]	**117.1**	110	120
Standard deviation of contact force σ[N]	**36.1**	32	40
Statistical maximum of contact force $F_m + 3\sigma$ [N]	**225.4**	210	230
Statistical minimum of contact force $F_m - \sigma$ [N]	**8.9**	–5	20
Actual maximum of contact force F_{max} [N]	**199.4**	190	225
Actual minimum of contact force F_{min} [N]	23.3	30	55
Percentage of loss of contact [%]	**0.0**	0	
Maximum uplift at support [mm]	66.3	55	65
Values within the standard limits are marked in bold. Values which exceed the limits are marked in italics.			

[Own study].

demonstrates reliability of the developed simulation method and its usefulness to predict the dynamic behaviour of the newly designed catenaries, in different operational conditions.

Literature

1. Ambrósio J., Pombo J., Pereira M. et.al.: A computational procedure for the dynamic analysis of the catenary-pantograph interaction in high-speed trains, Journal of Theoretical and Applied Mechanics, Vol. 50 (3), 2012, pp. 681–699.
2. Bryja D., Popiołek A.: Analiza drgań wieszara cięgnowego jako modelu kolejowej sieci trakcyjnej obciążonej ruchem pantografów, Journal of Civil Engineering, Environment and Architecture, Vol. 34, z. 64, No 2, 2017, pp. 177–190.
3. Bryja D., Popiołek A.: Analiza wpływu odległości między pantografami na drgania kolejowej sieci trakcyjnej, Archiwum Instytutu Inżynierii Lądowej, No 25, 2017, pp. 75–85.
4. Bryja D., Popiołek A.: Wstępna walidacja metody symulacji oddziaływania dynamicznego pomiędzy pantografem a siecią jezdną górną kolejowej trakcji elektrycznej, Przegląd Komunikacyjny, Vol. 72, No 6, 2017, pp. 21–27.
5. Bryja D., Prokopowicz D.: Dyskretno-ciągły model obliczeniowy sprzężonego układu dynamicznego: pantograf – napowietrzna sieć trakcyjna, Przegląd Komunikacyjny, Vol. 71, No 5, 2016, pp. 44–51.
6. Cho Y.H.: Numerical simulation of the dynamic responses of railway overhead contact lines to a moving pantograph, considering a nonlinear dropper, Journal of Sound and Vibration, No. 315, 2008, pp. 433–454.
7. Frýba L.: Dynamics of railway bridges, Academia Praha 1996.
8. Judek S., Karwowski K., Mizan M., et.al.: Modelowanie współpracy odbieraka prądu z siecią trakcyjną, Przegląd Elektrotechniczny, Vol. 91, nr 19, 2015, pp. 248–253.
9. Kaniewski M.: Symulacja uniesienia przewodów jezdnych sieci trakcyjnej pod wpływem przejazdu wielu pantografów, Czasopismo Techniczne. Elektrotechnika, Wydawnictwo Polititechniki Krakowskiej, Vol. 108, z. 13, 2011, pp. 143–153.
10. Langer J.: Dynamika budowli, Wydawnictwo Politechniki Wrocławskiej, Wrocław, 1980.
11. Massat J-P., Laurent Ch., Bianchi J-P., Balmes E.: Pantograph catenary dynamic optimisation based on advanced multibody and finite element co-simulation tools, Vehicle System Dynamics, Vol. 52 (1), 2014, pp. 338–354.
12. PN-EN 50318: Zastosowania kolejowe – Systemy odbioru prądu – Walidacja symulacji oddziaływania dynamicznego pomiędzy pantografem a siecią jezdną górną, PKN, Warszawa 2003.
13. Pombo J., Antunes P., Ambrósio J.: Recent developments in pantograph-catenary interaction modelling and analysis, International Journal of Railway Technology, Vol. 1 (1), 2012, pp. 249–278.
14. Wątroba P., Duda S., Gąsiorek D.: Symulacje numeryczne zjawisk dynamicznych w układzie pantograf – sieć jezdna, Modelowanie Inżynierskie, No 54, 2015, pp. 94–100.